NUMERICAL SIMULATION OF THE UNSTEADY AERODYNAMICS IN AN AXIAL COUNTER-ROTATING FAN STAGE

Mohand Younsi, B. Hutchinson, Florent Ravelet, Sofiane Khelladi, Farid Bakir

NUMERICAL SIMULATION OF THE UNSTEADY AERODYNAMICS IN AN AXIAL COUNTER-ROTATING FAN STAGE

Younsi M.* and Hutchinson B.
*Author for correspondence
ANSYS, Inc.
15 place Georges Pompidou
78180 Montigny le Bretonneux
France
E-mail : mohand.younsi@ansys.com

Ravelet F., Khelladi S. and Bakir F.
DynFluid Laboratory
151 boulevard de l'Hôpital
75013 Paris
France

ABSTRACT

The purpose of this work is to investigate and to understand the unsteady flow behavior in axial counter-rotating fan stage.
3D numerical simulations combined with experimental investigations were carried out, taking into account the entire environment of the stage. The numerical results were compared to the measurement data in terms of overall performance and local unsteady variables.
In the numerical procedure, the complete geometric details of the fan stage were taken into account, such as tip clearances, motor casings, etc. enabling an accurate presentation of the complex unsteady flow.

INTRODUCTION

The counter-rotating rotor configuration provides a way to design high performance and compact turbomachines for various industrial applications. It has been already applied in the areas of subsonic fans, pumps and turbines [1 - 4]. Compared with a traditional rotor-stator stage, the rear rotor in a counter-rotating stage is used not only to recover the static head but also to supply energy to the fluid. Therefore, to achieve the same performance, the use of a counter-rotating stage may lead to a reduction of the rotational speed and may generate more homogeneous flow downstream of the stage.
On the other hand, the mixing area between the two rotors induces complicated interacting flow structures [4]. The understanding of this highly unsteady flow in the mixing area is an open problem.
Moreover, the design method of such machines is still not sophisticated, due to a lack of systematic studies on the influence of free parameters, such as the distribution of loading, the axial distance, and the ratio of the rotation rates. The DynFluid laboratory has developed a design methodology for counter-rotating axial fans [4] and currently works on the influence of different design parameters [5].

Computational Fluid Dynamics (CFD) for 3D viscous flow fields provides an efficient tool for analysis, design and optimization. There is a continuously increasing demand in all areas of CFD for steady or unsteady flow simulations. In the turbomachinery area, the unsteady behavior of the flow field can have a significant influence on the aerodynamic performances and the acoustic behavior.
As a complementary or alternative approach to experimental methods, CFD analysis provides a viable way to understand the interactions and the flow unsteadiness in rotating machinery.
Previous works with CFD tools were realized in order to study counter-rotating configurations for fans, propellers, pumps and turbines, etc.
Numerical approaches were employed [6, 7] to study the flow field in a counter-rotating open rotors used in propulsion systems. The complexity of the unsteady flow induced by the interactions between the rotating blades was highlighted.
As the far field acoustic behavior depends on the flow unsteadiness, the CFD results showed that the most critical region for acoustics purposes is at the two rotors and the wake regions. Flow between the front and rear rotors is of particular interest as there is a subsequent phenomenon of fluid being continually "twisted" and "untwisted" by the counter-rotating front and aft rotors respectively, causing a potent area for waveform fluctuations causing disturbances in the audible range.
Other investigations were dedicated to ducted configurations. The impact of the blade pitch angles and the axial spacing between the counter-rotating propellers was investigated numerically [8].

NOMENCLATURE

BEP	[-]	Best Efficiency Point
BPF	[Hz]	Blade Passing Frequency
FR	[-]	Front Rotor
nf_{FR}	[Hz]	Harmonics of Front Rotor
mf_{RR}	[Hz]	Harmonics of Rear Rotor
RR	[-]	Rear Rotor
R_{hub}	[mm]	Hub blade radius
R_{tip}	[mm]	Tip blade radius
S	[mm]	Axial distance between FR and RR
Zp	[mm]	Axial position

NUMERICAL SIMULATION PROCEDURE

In this paper, 3D numerical simulations were carried out using the commercial CFD code ANSYS CFX release 16.2. The flow solver is a coupled pressure-based solver. It employs a fully implicit solution strategy. The focus of this work is transient CFD simulations. However, steady calculations were also performed to predict the overall performance and to initialize the unsteady calculations.

The steady method uses a mixing plane type of approach called a "Stage Interface" where momentum and energy are conserved across the interface, but entropy increases as a result of the circumferential averaging process. This steady method requires simulation of only one blade per row.

The unsteady calculations use the Transient Rotor-Stator (TRS) approach where the true change in relative position of the front rotor and rear rotor are accounted for within fully implicit interface discretization. In this approach, either full wheel is assumed or the smallest possible circumferential sector with an integer number of blades, according to the pitch ratio, is modelled with standard periodicity applied to the blade ensemble (unity ensemble pitch ratio between blade rows).

In this work, the blade counts were such that it was necessary to model the full wheel to achieve unity pitch ratio.

Geometry and Mesh

Figure 1. shows the axial counter-rotating stage geometry and its main characteristics are summarized in Table 1.

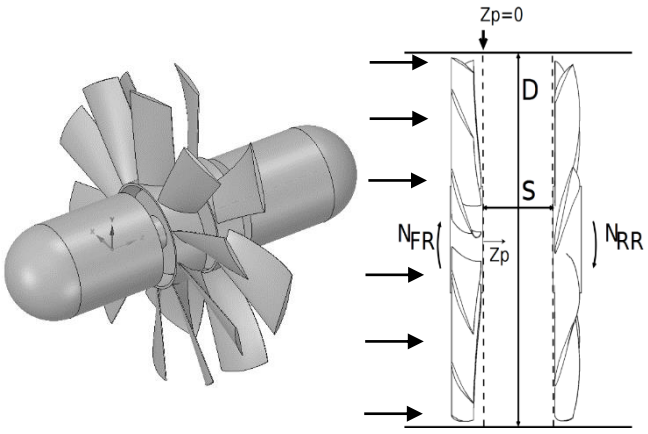

Figure 1 Geometry of the counter-rotating fan

	FR	RR
R_{tip} *[mm]*	187.5	
R_{hub} *[mm]*	65	
Tip Clearance [mm]	2.5	
Blades Count	10	7
Rotational Velocity [rpm]	-2300	2200
Blade Passing Period [s]	0.0026	0.0039
BPF [Hz]	383.33	256.66

Table 1 Main characteristics of the axial counter-rotating fan

The entire geometry features, including tip clearance, were taken into account in the meshing procedure. The bladed fluid domains were meshed using the ANSYS TurboGrid software. Elsewhere, ANSYS Meshing software was used to mesh the upstream domain, the downstream domain and the motor casings. One and one half million cells were used for each of the FR and RR domain sectors, thus the full computational domain consists of three million cells.

Particular attention was devoted to the mesh distribution in the boundary layers and the tip clearance. Ten cells were imposed in the radial gap between the blade tip and the shroud. The near-wall mesh was adapted to the boundary layer flow. The dimensionless wall distance y^+ stands in the range [3 - 8]. Figure 2 illustrates the resulting hexahedral mesh and Figure 3 shows the mesh details for the FR blade domain.

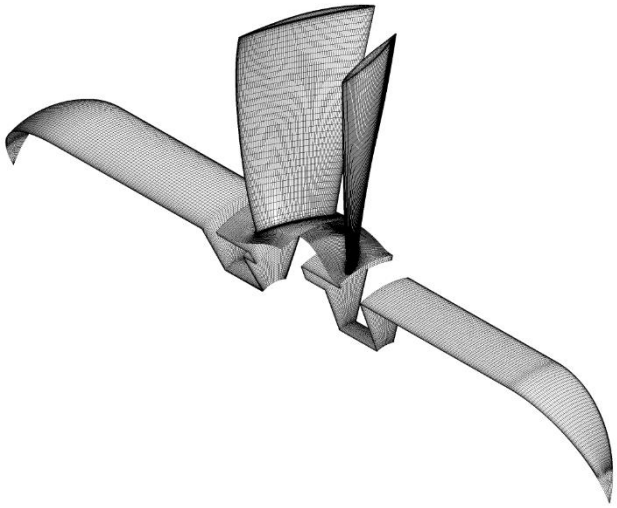

Figure 2 Overview of the periodic domain mesh

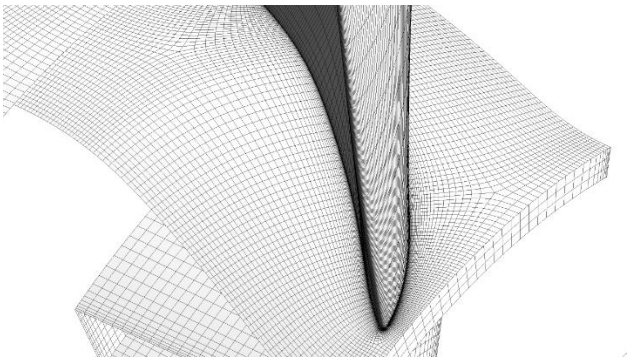

Figure 3 Mesh details for the FR blade domain

Simulation Parameters and Setup

The numerical simulations (steady and unsteady) were performed at the design point of the fan which corresponds to a pressure rise of 363 Pa and a mass flow rate of 1.2 kg/s.

A first steady simulation was performed with total pressure and mass flow boundary conditions at the inlet domain and the outlet domain respectively. Only one blade pitch for each rotor was simulated with rotational periodic boundary conditions. The

Shear-Stress Transport k-Omega model [9] was used for the turbulence modelling. The air is assumed incompressible.
The second step of the simulation procedure was focused on the unsteady calculations. The previous mesh was duplicated in order to obtain a full wheel grid mesh of 27 million cells.
Total pressure and static pressure were used as boundary conditions at the inlet and the outlet domain respectively. A time-step of 3.26 E-5 seconds was chosen and it corresponds to 80 time-steps per FR blade passing period (a rotation of -0.45 degrees) and 120 time-steps for RR blade passing period (a rotation of 0.43 degrees). The unsteady simulations were initialized by the steady calculations results.

EXPERIMENTAL WORK

The experimental investigations were performed in a test rig, built according to the ISO-5801 standard [ref.]. A schematic diagram of test rig is shown in Figure 4. First, the air comes into the test pipe through a bell mouth, then passes through the driving motor of the Front Rotor, and is homogenized by a honeycomb. Next, energy is transferred to the fluid by the Counter-Rotating Stage. The axial distance between FR and RR can be modified by a series of blocks. Then, the flow passes the driving motor of the RR and an anti-gyration device to remove the rotational component of the flow, before the measurement of the static pressure by 4 pressure taps. After that, the fluid goes through an ISO-5167 orifice plate in order to measure the volume flow rate. Finally, the fluid is regulated by an axial blower and an iris damper before being discharged into the ambient atmosphere. The uncertainties of the measurements were evaluated in previous work [4].

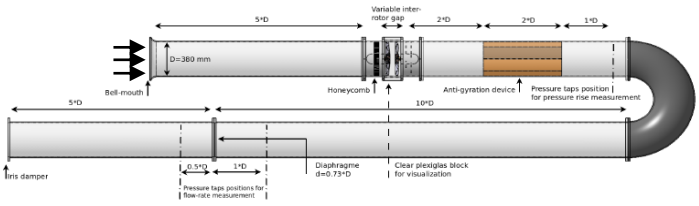

Figure 4 Schematic of test rig

Velocity Components Measurements

In addition to overall performances measurements, Laser Doppler Velocimetry (LDV) measurements were conducted at three axial positions in the counter-rotating fan stage: Upstream of the FR (Zp = -46), between the FR and the RR (Zp = 5) and downstream of the RR (Zp = 50). At each axial position, velocities were measured on 25 radial positions from hub to shroud as shown in Figure 5.
The measured instantaneous velocities were time-averaged circumferentially at a given radial and axial position and accordingly, the CFD results will be circumferentially averaged.

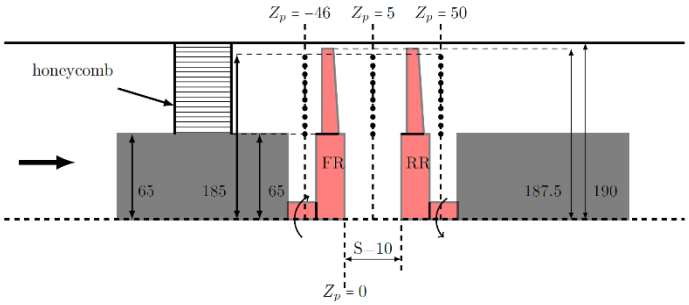

Figure 5 Axial and radial positions of LDV measurements

Wall Pressure Fluctuations Measurements

The wall pressure fluctuations are measured by a flush-mounted pressure microphone calibrated by an acoustic calibrator. This microphone is placed at the top of the block of the fan stage and between the two rotors (Figure 6). The sampling frequency for the signal is 6 kHz. Then the Power Spectral Density (PSD) of the signal is calculated.

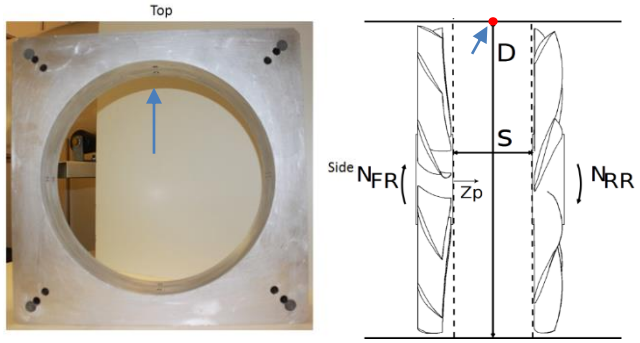

Figure 6 Flush-mounted microphone position

NUMERICAL AND EXPERIMENTAL RESULTS

Figure 7 (top) shows the blade-to-blade absolute velocity contour at mid-span obtained with the steady approach. The blade wakes generated by the FR can be observed until the interface with the RR domain where the variables are averaged. At the bottom of the figure, unsteady results give more details on the complex flow and the interactions between the FR and RR are illustrated.

Upstream of the stage, where the interactions are small, the velocity contours are similar between the steady and the unsteady solutions. However, at the interface between the two rotors and particularly at the downstream of the domain, the interactions are highlighted by the unsteady simulations. The wakes generated by the counter-rotating blades are crossing with each other's. This wake combination process has an effect on the unsteady signals and their corresponding frequencies.

The spectral analysis of the temporal signals recorded at strategic locations in the flow domain will enable study of the different frequencies related to the unsteady interactions.

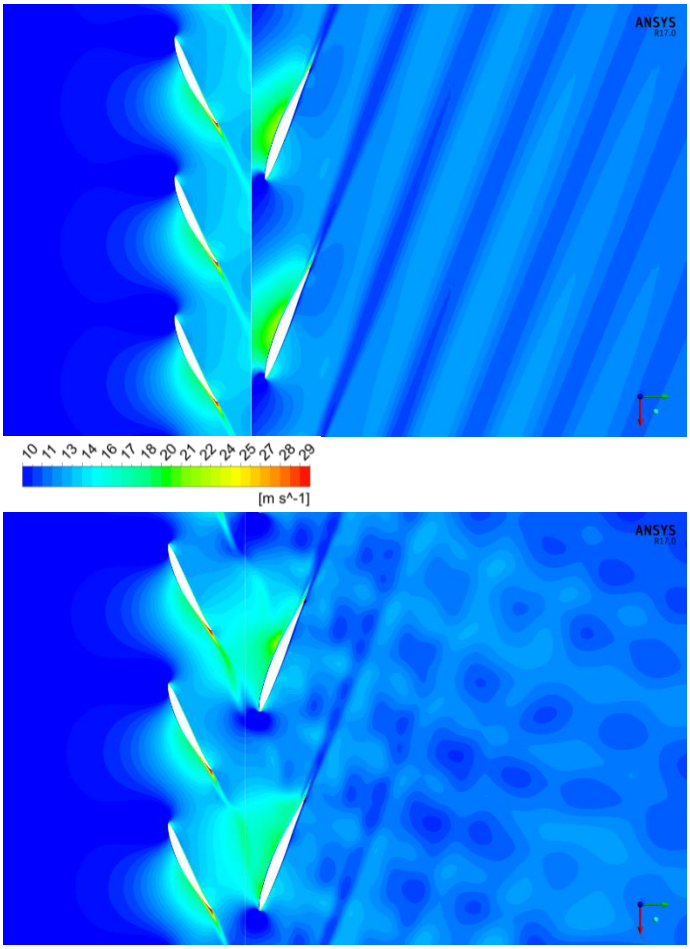

Figure 7 Blade-to-blade absolute velocity at mid-span (top: steady, bottom: unsteady)

Overall Performance

Table 2 gives a comparison between the overall performance obtained numerically (steady state) and experimentally at the BEP of the counter-rotating fan. It can be seen that the global performance is well predicted by the steady numerical approach. The unsteady calculations give similar results.

	Experiment	ANSYS CFX
Pressure Rise [Pa]	363 ± 4	365
Static efficiency[%]	66.1 ± 1.4	64
FR power [W]	335 ± 2.5	327

Table 2 Overall performance at the BEP

Radial Distribution of Velocity Components

The time-averaged velocity profiles given by the unsteady calculations were compared to LDV measurements. Figure 8 shows the radial distribution of the absolute circumferential velocity at Zp = -46, Zp = 5 and Zp = 50 planes. The curves at the upstream of the fan stage (Zp = -46) demonstrate clearly that the flow comes without pre-rotation. The mean value is around 0 m/s. However, a particular behavior can be observed at the tip blade zone which is due to the tip leakage phenomena.

Good agreement between the numerical and the experimental data can be observed.

According to Figure 9 and due to the radial equilibrium condition, the axial velocity profiles are globally conserved from the upstream to the downstream domain.

The analysis of the absolute circumferential velocity profiles at the three locations shows that the rear rotor plays an important role to reorient the flow axially at the exit domain. Thus, at Zp = 50 plane, the mean circumferential velocity magnitude is very small. This result confirms the preliminary design objective of achieving low swirl at the exit of the counter-rotating fan stage.

Some LDV velocity measurements reveal that some strong modifications of the flow close to the hub and to the blade tip [5] seem to take place, in regions where it is difficult to have access experimentally. That could explain the discrepancies between the numerical model and the measurements at these zones.

Wall Pressure Fluctuations

The wall pressure fluctuations and its corresponding spectrum are illustrated in Figure 10. The signal corresponds to 5 FR revolutions time-signature. Experiment and CFD results show excellent agreement, especially the full 3D unsteady simulations that succeed in reproducing most of the spectral peaks, including the blade passing frequency of the FR, of the RR, and their harmonics and interactions. The pressure spectrum clearly distinguishes the linear combination of different modes which are the result of the unsteady flow interactions between the two rotors (peaks at f_{FR}, f_{RR}, $n.f_{FR}$, $m.\ f_{RR}$ $n.f_{FR}+m.\ f_{RR}$,..).

Velocity Fluctuations

Figure 11 presents the velocity fluctuations at Zp = 5 plane. The point of interest is located at 120 mm radially from the rotational axis.

The velocity fluctuation amplitude stands in the range of [-3.5, 3.5] m/s. Some discrepancies can be noticed between the numerical and the experimental results. The measurement procedure used here shows some limitations to accurately capture the velocity fluctuations. More efforts have to be considered in the future to analyse and improve the measurement accuracy.

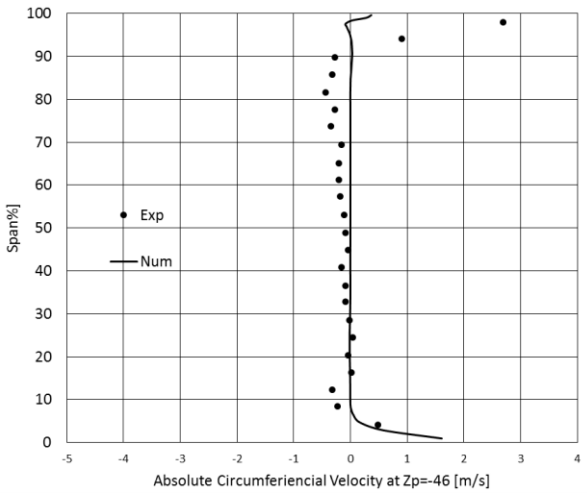

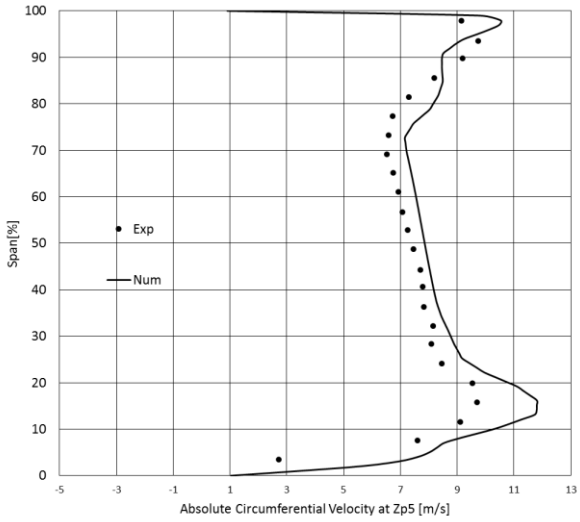

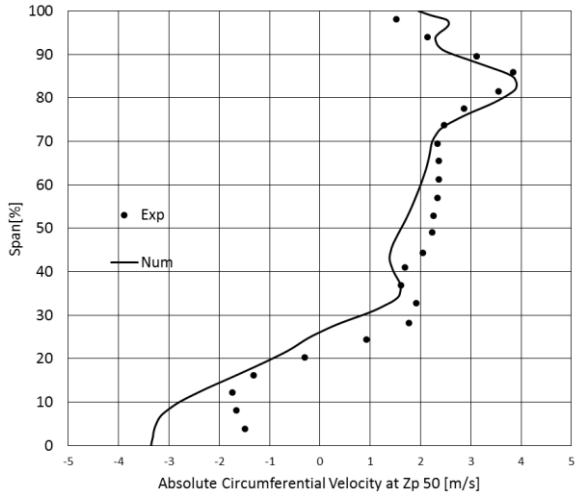

Figure 8 Radial distribution of absolute circumferential velocity

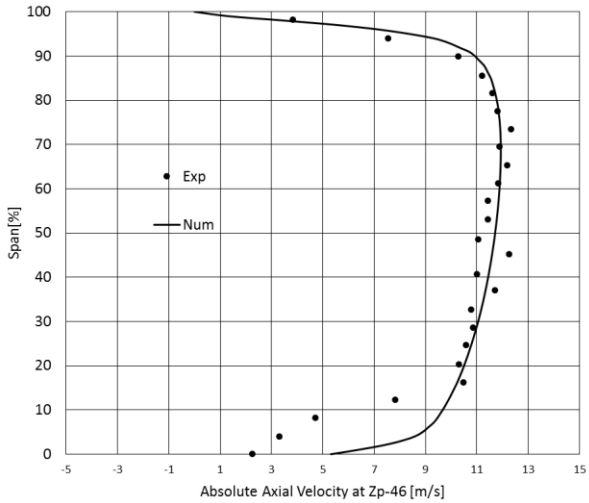

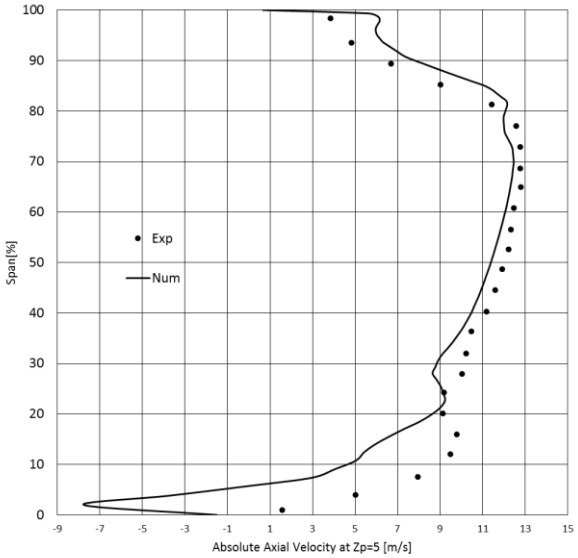

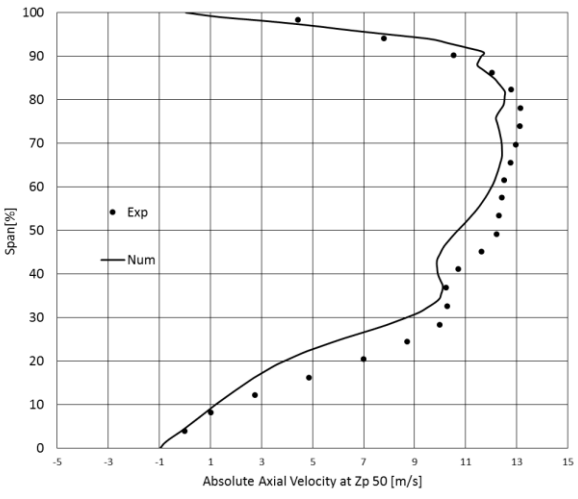

Figure 9 Radial distribution of axial velocity

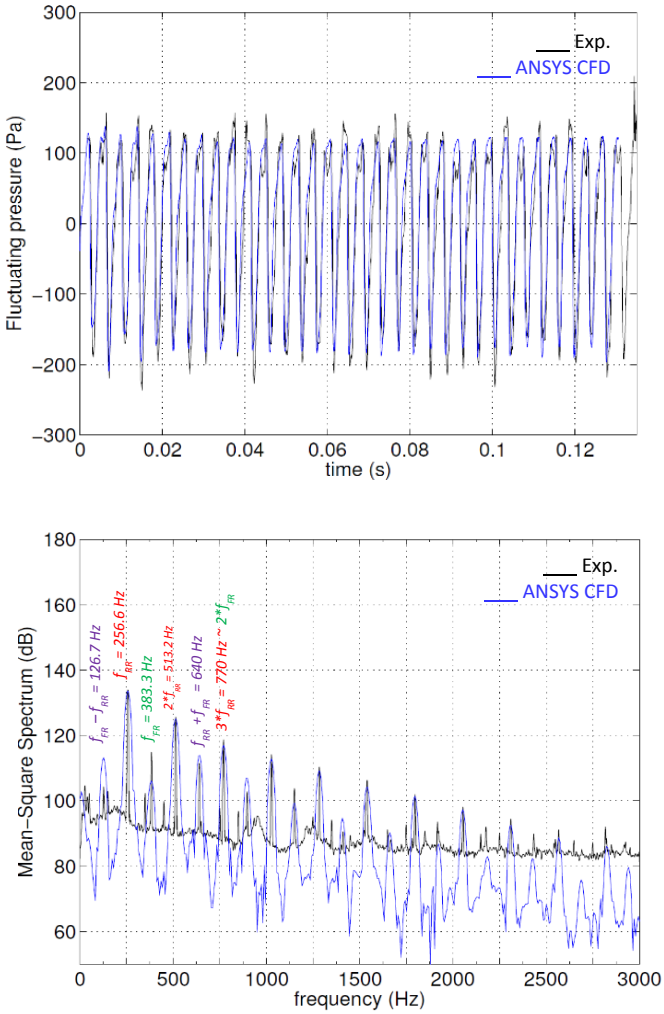

Figure 10 Wall pressure fluctuations and its spectrum

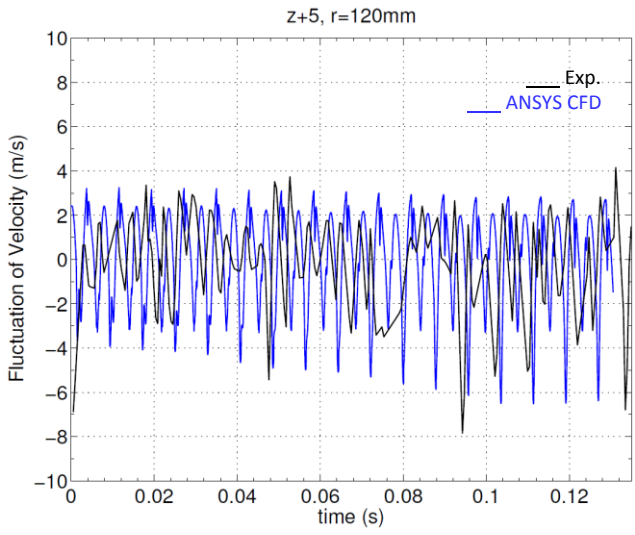

Figure 11 Velocity fluctuations at Zp = 5

CONCLUSION

Unsteady flow through an axial counter-rotating fan stage was studied and investigated using ANSYS CFX in this work. The numerical procedure was compared locally and globally to experimental data. The complete geometry details of the fan stage were taken into account, such as tip clearances, motor casings, etc. contributing to an accurate representation of the complex unsteady flow. Good agreement between numerical and experimental results was observed.

It should be interesting to extend this study in the future by:

- Studying and optimizing the impact of the axial distance between the two rotors on the internal flow and the acoustic behaviour
- Acoustic measurements at the far field in an anechoic room to avoid sound reflections.
- Further analysis in order to better understand the coupling of the two rotors, i.e. the effects of the presence of the Rear Rotor onto the Front Rotor. Some measurements of velocity with LDV have indeed revealed that some strong modifications of the flow close to the hub and to the blade tip seem to take place, in regions where it is difficult to access experimentally. The use of Scale-Resolving Simulations (SRS) models available in ANSYS CFX should give more information.

REFERENCES

[1] Shigemitsu, T., Furukawa, A., Watanabe, S., Okuma, K., and Fukutomi, J., Internal flow measurement with LDV at design point of contra-rotating axial flow pump, *Journal of Fluid Science and Technology*, Vol. 4, 2009, p. 723-734

[2] Joly, M., Verstraete, T., and Paniagua, G., Full design of a highly loaded and compact contra-rotating fan using multidisciplinary evolutionary optimization, Proceedings of the ASME Turbo Expo 2013: Turbine Technical Conference and Exposition, San Antonio, Texas, USA, 2013

[3] Cho, L.S., Cha, B.J., and Cho, J.S., Experimental study on the three-dimensional unsteady flow characteristics of the counter-rotating axial flow fan, *Journal of Fluid Science and Technology*, Vol. 4, 2009, pp. 200-209

[4] Nouri, H., Danlos, A., Ravelet, F., Bakir, F., and Sarraf, C., Experimental study of the instationary flow between two ducted counter-rotating rotors, *Journal of Engineering for Gas Turbines and Power*, Vol. 135, 2013, pp. 022601

[5] Wang, J., Ravelet, F., and Bakir, F., Influence of design parameters on the global performances of low-speed counter-rotating axial-flow fans. *American Society of Mechanical Engineers, Fluids Engineering Division*, 2014, paper FEDSM2014-22717.

[6] Roosenboom E.W.M., Schröder, A., Geisler, R., Pallek, D. and Agocs, J. Experimental and numerical investigation of a counter rotating open rotor flow field, *29th AIAA Applied Aerodynamics Conference*, 2011, Honolulu, Hawaii

[7] Farooque, M. S., CFD grid generation and flow analysis of a counter-rotating open rotor propulsion system, Thesis, Ohio State University, 2010.

[8] Xu, C., Bil, C., and Cheung, S.C.P, Fluid dynamics analysis of a counter –rotating ducted propeller, *29th Congress of the International Concil of the Aeronautical Sciences*, 2014, Petersburg, Russia.

[9] Menter, F.R., Two-equation eddy-viscosity turbulence models for engineering applications, *AIAA-Journal.*, Vol. 32, 1994, pp. 1598-1605